Trends and drivers in global surface ocean pH over the past three decades

S. K. Lauvset[1,2]; N. Gruber[3]; P. Landschützer[3]; A. Olsen[1,2,4]; J. Tjiputra.[2,4]

[1]Geophysical Institute, University of Bergen, Norway

[2]Bjerknes Center for Climate Research, Bergen, Norway

[3]Environmental Physics, Institute of Biogeochemistry and Pollutant Dynamics, ETH Zurich, Zürich, Switzerland.

[4]Uni Climate – Uni Research, Bergen, Norway

Correspondence to S. K. Lauvset (siv.lauvset@gfi.uib.no)

Abstract

We report global long-term trends in surface ocean pH using a new pH data set computed by combining fCO_2 observations from the Surface Ocean CO_2 Atlas (SOCAT) version 2 with surface alkalinity estimates based on temperature and salinity. Trends were determined over the periods 1981-2011 and 1991-2011 for a set of 17 biomes using a weighted linear least squares method. We observe significant decreases in surface ocean pH in ~70% of all biomes and a mean rate of decrease of 0.0018±0.0004 yr^{-1} for 1991-2011. We are not able to calculate a global trend for 1981-2011 because too few biomes have enough data for this. In half the biomes, the rate of change is commensurate with the trends expected based on the assumption that the surface ocean pH change is only driven by the surface ocean CO_2 chemistry remaining in a transient equilibrium with the increase in atmospheric CO_2. In the remaining biomes deviations from such equilibrium may reflect that the trend of surface ocean fCO_2 is not equal to that of the atmosphere, most notably in the equatorial Pacific Ocean, or changes in the oceanic buffer (Revelle) factor. We conclude that well-planned and long-term sustained observational networks are key to reliably document the ongoing and future changes in ocean carbon chemistry due to anthropogenic forcing.

1. Introduction

The concentration of atmospheric carbon dioxide (CO_2) is rapidly increasing due to the burning of fossil fuels, cement production, and land use changes (Le Quéré et al., 2014).

This drives a net flux of CO_2 into the ocean, causing the dissolved inorganic carbon (DIC) concentration to increase, which drives a decrease in pH and in the concentration of the carbonate ion (CO_3^{2-}, Doney et al., 2009b; Zeebe and Wolf-Gladrow, 2001). These changes in the ocean inorganic carbon chemistry, collectively referred to as ocean acidification (Gattuso and Hansson, 2011), are a source of concern due to their potential impact on organisms, ecosystems and biogeochemical cycles (Doney et al., 2009a). Hereafter we refer to the inorganic carbon chemistry in the ocean as CO_2 chemistry. In contrast to the surface ocean fugacity of carbon dioxide (fCO_2), for which many studies have analyzed the long-term trends, both regionally and globally (*e.g.* Fay and McKinley, 2013; Le Quéré, 2010; Lenton et al., 2012; Takahashi et al., 2009b), only a handful of regional studies have so far been published on long-term pH trends (Bates, 2007; Dore et al., 2009; Gonzalez-Davila et al., 2007; Olafsson et al., 2010).

The most extensive assessment to date is the one of Bates et al. (2014). They described changes in ocean CO_2 chemistry variables at seven, mostly tropical/sub-tropical, time-series stations, all of which have been occupied for at least two decades. Their analysis shows that while there are regional differences, these open ocean time-series show relatively similar trends in DIC, fCO_2, and pH. At the tropical and subtropical open ocean stations (Bates, 2007; Dore et al., 2009; Gonzalez-Davila et al., 2010) ocean pH is decreasing at a rate of 0.0017 ± 0.0002 yr^{-1}. At the high-latitude stations, however, a more variable picture emerges. While the pH trend in the Icelandic Sea follows the rate observed at the lower latitude stations, the trend in the Irminger Sea (Olafsson et al., 2010) is nearly twice as large, *i.e.*, -0.0026 ± 0.0006 yr^{-1}. Thus, in a global analysis, we expect a complex spatial pattern of long-term trends, yet hitherto unknown.

The absence of a global analysis of long-term trends is largely a consequence of the lack of direct surface ocean pH measurements, which is in sharp contrast to the situation for surface ocean fCO_2, for which data products contain several million observations (Bakker et al., 2014; Pfeil et al., 2013; Takahashi et al., 2009a). This limitation can be overcome by using computed pH, obtained by combining the very large data products of fCO_2 with estimates of surface alkalinity. Lauvset and Gruber (2014) demonstrated for the North Atlantic that this approach is able to produce rather accurate estimates of surface ocean pH. Takahashi et al. (2014) came to the same result globally. Even though the use of pH computed from fCO_2 generates a global data set containing millions of pH observations, the resulting data are still sparse in time and space on a global scale, making the determination of

global long-term trends challenging. For surface pCO_2 this challenge has historically been overcome by binning the data into a very coarse grid (order of 5º-10° in latitude and longitude) by *e.g.* Lenton et al. (2012), Takahashi et al. (2002), and Takahashi et al. (2009b), but more recently Fay and McKinley (2013) proposed to aggregate the data into biomes. This type of aggregation is more likely to capture the correct long-term dynamics of a region, as one expects a biome to respond in a more coherent manner to perturbations than a region defined by a latitude/longitude range.

Given the absence of a global observation-based analysis of pH trends, models have so far been the only source of information. The Norwegian Earth System Model (NorESM1-ME), as part of the Coupled Model Intercomparison Project phase 5 (CMIP5, Taylor et al., 2012), simulates a global average pH decrease of 0.0017 yr^{-1} (1981-2011), which is largely commensurate with observations reported from the time series stations. A recent study using ten different CMIP5 models, including NorESM1-ME, showed that all models give similar global average pH trends—both in the historical and future scenarios (Bopp et al., 2013).

This secular pH trend of -0.0017 yr^{-1} and the low spread between models is expected for an ocean where (i) the surface ocean fCO_2 follows that in the atmosphere due to the sufficiently rapid exchange of the excess CO_2 between the atmosphere and the surface ocean, and (ii) where the change in the buffer (Revelle) factor remains spatially uniform, as the partial derivative $\partial[H^+]/\partial fCO_2$ is directly related to this quantity (Orr, 2011; Sarmiento and Gruber, 2006). A change in the buffer (Revelle) factor is expected as much of the CO_2 newly added to the surface ocean from the atmosphere will be titrated away by CO_3^{2-}, causing a decrease in its concentration. This decreases the ability of the surface ocean to “buffer” the pH against further uptake of CO_2, thus increasing the Revelle factor (Sarmiento and Gruber, 2006). However, regional variations in how the Revelle factor changes may occur. Bates et al. (2014) show, for example, not only variations of the pH trends between the high- and low latitude time series, but also that the trends in Revelle factor are different, indicating that other factors are influencing the Revelle factor. These factors are mainly those processes that affect DIC and alkalinity, such as changes in ocean productivity and calcification, while changes in temperature and salinity are of minor importance (Sarmiento and Gruber, 2006).

Local and regional changes in the buffer (Revelle) factor are driven by the changing, and spatially varying, ratio of DIC to alkalinity. Spatial changes in this ratio have the potential to decouple the pH trends from those of the surface ocean fCO_2 (Orr, 2011), potentially causing a more variable pattern in the pH trends. The complex spatial variability, identified by

Bates et al. (2014) and others (*e.g.* Tjiputra et al., 2014) supports this hypothesis. This also shows that analyses of global pH trends, including the regional distribution of changes and the dynamics of the changing ocean CO_2 system, are required for a comprehensive understanding. Global analyses are also necessary for the validation of model results, for underpinning and interpreting response studies from organism to ecosystem level, and for optimizing the planning of continued and future observational networks.

Here we take advantage of the approach of Lauvset and Gruber (2014) to determine global ocean pH trends, and their drivers, using pH data calculated from the more than 10 million observations of surface ocean fCO_2 that have been made available through the Surface Ocean CO_2 Atlas (SOCAT) project (Bakker et al., 2014; Pfeil et al., 2013). Although pH is the main parameter of interest, fCO_2 has been carried through all our analyses in order to determine how CO_2 chemistry causes the evolution of pH to differ from that expected from fCO_2 alone. Finally we use the long term pH trends derived from a global earth system model, the NorESM1-ME, in order to illustrate how important spatial variability is for the representativeness of our trend results.

2. Data and Methods

We calculated pH in the surface ocean by a two-step calculation using observations of fCO_2, sea surface temperature (SST), and sea surface salinity (SSS) from SOCAT version 2, (Bakker et al., 2014). In the first step, alkalinity was calculated from SSS and SST using the algorithms developed by Lee et al. (2006) and Nondal et al. (2009). The Nondal et al. (2009) algorithms were developed specifically for the high-latitude (>60ºN) Atlantic Ocean, and were used only there. Whenever no measured SSS was available in the SOCATv2 data set the climatological World Ocean Atlas SSS value (Antonov et al., 2010)—which is included in the SOCATv2 data product—was used instead. The SOCAT SSS data have not been quality controlled and might therefore be biased. Lauvset and Gruber (2014) showed that this potential bias does not greatly affect the precision of the pH trends. It may affect the accuracy of the calculation, but for our purpose of determining long-term trends, the accuracy (*i.e.* the lack of bias in the data) is of less importance as long as the precision is good enough, and assuming that any bias remains constant over time. In the second step, pH on the total scale at *in situ* temperature was calculated from the estimated alkalinity and the observed fCO_2 using CO2SYS (Lewis and Wallace, 1998). We used the K_1 and K_2 constants from Mehrbach et al.

(1973) refit by Dickson and Millero (1987), and the borate to salinity ratio from Uppström (1974). Since we use CO2SYS this calculation also gives us dissolved inorganic carbon (DIC) and all other variables of the ocean carbon chemistry system.

Quite a few of the data fall outside the valid ranges for input data for the Lee et al. (2006) and Nondal et al. (2009) alkalinity algorithms and are lost in this step. There remain 7,381,013 data points of pH (and alkalinity) over the global ocean in the time period 1973-2011. The fCO_2 trends have been estimated using only data points which have a calculated pH value in order to avoid spurious differences when comparing these trends to those of pH. The global calculation error (precision) for pH is 0.0032±0.0005, and the calculated pH compares well to observed pH at crossover locations in the Atlantic Ocean (Lauvset and Gruber, 2014). Before analysis the pH data were bin averaged into monthly 1^ox1^o bins, using no extrapolation or interpolation of the data. The global data set was divided into the 17 ocean biomes, defined (using mixed layer depth, sea surface temperature, and chlorophyll-a concentrations) by Fay and McKinley (2014), as shown in Fig. 1. Here, we only evaluate trends in the open ocean. Data from coastal regions shallower than 250 m, based on the ETOPO2 bathymetry, and those with salinity <20 were removed.

In each biome a least squares linear regression weighted with Tukey's bisquare method was used to determine the long-term pH trend. For the long-term trend determination we required each biome to have at least three observations in each decade (1981-1990, 1991-2000, and 2001-2011). While this criterion was met in only 8 biomes for the period 1981-2011, 15 had sufficient data for the period 1991-2011. Both ordinary and weighted least squares regressions were carried out, but we chose a weighted least squares regression over an ordinary least squares regression since this is less sensitive to outliers in the data. This makes the statistics of the regression more robust, but generally this choice does not significantly affect the results presented here. All regression results are presented with the standard error of the slope (se), which represents its 68% confidence interval, and the root mean square error (RMSE). The RMSE is used as a measure of interannual variability.

Before the regression analysis was carried out two corrections were applied to the data: deseasonalization and removal of spatial bias. The importance of these corrections, particularly in data sparse biomes such as those in the Southern Ocean, was recently highlighted by Fay et al. (2014). The seasonal cycle in the data was removed following Takahashi et al. (2009b), using the long-term average seasonal cycle as contained in our data for each biome. However, we find that using the climatological seasonal cycle—calculated

using the Takahashi pCO_2 climatology (Takahashi et al., 2009a)—does not significantly affect the results. To correct for any spatial bias in the large scale biomes the difference between the climatological value in each 1°x1° bin and the biome mean climatological value was subtracted from the observed value in each 1°x1° bin. There is no difference between this method and simply subtracting the climatological value in each 1°x1° bin, but our approach retains the absolute values in each biome. It should be noted that the computed trends in some biomes are sensitive to which climatological data is used for the spatial bias correction: subtracting the climatological value vs. subtracting the long-term average in each 1°x1° bin. Mostly this is because in some 1°x1° bins, the long-term average is biased towards the last decade, which has significantly more data than earlier periods.

A statistical test was performed to test the necessity of these corrections: results after applying one or both corrections were compared to results after applying none using a one-way analysis of variance (ANOVA, see *e.g.* Vijayvargiya, 2009). A statistically significant change in the slope and its standard error was interpreted as making the correction(s) necessary. The deseasonalization removes scatter in the data and leads to more robust regressions by reducing the standard error of the slope in all biomes. This correction does not significantly (p-value<0.05) affect the long-term trend in any biome or time period, however. The spatial bias correction has no statistically significant impact on the long term trend in most biomes, but because it reduces the standard error and increases the r^2 in six biomes we decided to keep it applied. The long-term pH trend is also much more sensitive to this correction than the fCO_2 trend, mostly because the pH trend is very small and thus more sensitive to any data correction.

The pH change expected from a certain change in fCO_2 was calculated using $\Delta pH/\Delta fCO_2 = \partial pH/\partial fCO_2$. The partial derivative was estimated in CO2SYS using 0.01 μatm increments in fCO_2. Since both the fCO_2 and pH trends are inextricably coupled to DIC change, what we in reality calculate here is the pH change incurred by a change in DIC equivalent to the given fCO_2 trend when alkalinity, SST, and SSS remain constant. We used the same equation to evaluate what global average fCO_2 change the global long-term trend in pH is consistent with, but then using -0.001 incremental changes in pH.

In each biome the long-term trend in pH was decomposed into the effects of changes in SST, SSS, alkalinity, and DIC. First the impact of each of these drivers on the fCO_2 trend was determined following Takahashi et al. (1993), equations 2-5, we then converted our results to the impacts on $[CO_2]$ and on $[H^+]$ following equation 1.5.87 in Zeebe and Wolf-

Gladrow (2001), and finally we determined the impact on pH. The DIC data and dissociation constants required for these calculations were calculated in CO2SYS from the fCO_2 and alkalinity pair in the same calculation that gave us pH.

To test the effect of the highly variable spatial and temporal coverage of the observational data on the results we have used the NorESM1-ME Earth system model, which prognostically simulates the seawater CO_2 chemistry. A detailed description and evaluation of the model simulation is available in Tjiputra et al. (2013). We examined the model simulation for the 1981-2011 period based on the CMIP5 historical and future RCP8.5 scenarios, where the atmospheric CO_2 concentration is used as the boundary condition. We binned the model monthly output into the same 1ºx1º bins and used the same method to calculate and decompose the long-term trends in each biome as we used for the observational data—including the two-step pH calculation described above. Two sets of model trends were determined. For the first, we used the fully sampled model output, referred to here as the 'fully-sampled trend'. For the second set, we subsampled the model output according to the observational coverage, *i.e.* only data from monthly grid cells corresponding to those where real observations have been obtained were used. The 'sub-sampled trend' was then computed from these subsampled model data. The comparison of these two informs us on how sensitive the calculated trends are to the variable data coverage.

3. Results and Discussion

3.1. Long-term trends in pH

We find statistically significant trends in 6 out of the 8 biomes with sufficient data for the period 1981-2011, and for 13 out of the 15 biomes with sufficient data for the period 1991-2011 (Fig. 1 with the numerical values in Table 1). As shown in Figs. 2-4, the data coverage in each biome is generally very good after 1990, but often spotty prior to this year. These figures also reveal a substantial amount of interannual variability around the determined trends, with RMSE values of between 0.01 and 0.04 pH units— *i.e.*, roughly of similar magnitude as the cumulative trend over the 20 to 30 years of analyses. No robust analyses were possible for the North Pacific ice covered (NP-ICE) and North Atlantic ice covered (NA-ICE) biomes, due to the lack of data (<20 data points) hence they are not further

discussed in the paper. Unfortunately, these are the Arctic biomes where the earliest impacts of ocean acidification are expected (Steinacher et al., 2009).

The regions with sufficient data, but without statistically significant trends, *i.e*, the North Pacific subpolar seasonally stratified (NP-SPSS) biome for the period 1981-2011, and the Southern Ocean subtropical seasonally stratified (SO-STSS) and ice covered (SO-ICE) biomes for the period 1991-2011, are characterized by large RMSE and a substantial amount of decadal variability, which is likely masking the long-term trends. In addition to these three biomes where the trends are statistically indistinguishable from zero, the South Pacific subtropical permanently stratified (SP-STPS) biome is likely biased by its low data density, and will not be further discussed. This decision was corroborated by comparing the pH trend in the fully-sampled model results with the sub-sampled model results (Fig. 5): the SP-STPS biome is the only one where the difference in these trends is statistically significant at the 95% confidence level.

Since we are not able to calculate statistically significant trends in all 17 biomes we are also unable to calculate a global average trend. For the period 1991-2011 only the Arctic and parts of the Southern Ocean have no statistically significant results, and the area-weighted average pH decrease of the remaining 13 biomes (Table 1), is 0.0018±0.0004 yr^{-1}. For the period 1981-2011 the number of biomes with trend estimates is quite small, but almost all the Pacific Ocean biomes have results and the area-weighted pH decrease is 0.0019±0.0001 yr^{-1} between 1981 and 2011. Within the uncertainty limits the global 1991-2011 trend is comparable to the global trend in the fully-sampled NorESM1-ME model results (-0.0017 yr^{-1}) and to the average trend of -0.0018±0.0003 yr^{-1} over the seven time series evaluated by Bates et al. (2014). Assuming that alkalinity, SST, and SSS remain constant, and that the change in DIC and Revelle factor remains spatially uniform, this global average pH trend corresponds to a rate of increase in surface ocean fCO_2 of 1.75±0.4 μatm yr^{-1}, which is roughly the rate of increase in atmospheric fCO_2. Regionally, however, the response of the ocean CO_2 system to the atmospheric forcing is more variable (Fig. 1).

In the North Atlantic subpolar seasonally stratified (NA-SPSS) biome the observed pH trend is -0.0020±0.0004 yr^{-1}. This is right in between the trend observed at the Irminger Sea time series (-0.0026±0.0006 yr^{-1}) and that observed at the Iceland Sea time series (-0.0014±0.0005 yr^{-1}) (Bates et al., 2014). Within the 68% confidence intervals, the NA-SPSS pH trend is consistent with both of these local trends. In the North Atlantic subtropical seasonally stratified (NA-STSS) biome there are no time series data to compare with, but its

trend of -0.0018±0.0003 yr^{-1} is consistent with a trend of ~ -0.0020 yr^{-1} observed in the Rockall Trough by McGrath et al. (2012). In the North (NA-STPS) and South (SA-STPS) Atlantic subtropical permanently stratified biomes the pH trend is the same, but the RMSE values indicate larger interannual variability in the southern biome (Table 1). This is likely caused by the inclusion of the Benguela upwelling region, but the full effect of this has not been quantified for the SA-STPS or any other biome. The trend identified here for the NA-STPS (-0.0011±0.0002 yr^{-1}) is significantly lower than the trend observed at the Bermuda Atlantic Time-series Study (BATS, Bates et al., 2014), of -0.0017±0.0001 yr^{-1}. Unfortunately, we have no time series data for comparison in the SA-STPS biome. In the Atlantic Ocean equatorial region (A-EQU) the pH trend (-0.0016±0.0003 yr^{-1}) is lower than that observed at the Carbon Retention in A Colored Ocean (CARIACO) time-series station of -0.0025±0.0004 yr^{-1} (Bates et al., 2014), but this station is located at the very edge of the biome in a more coastal setting and not ideal for comparison.

In the Pacific Ocean the RMSE around the fitted pH trends is generally larger than in the Atlantic Ocean (Table 1), possibly reflecting the higher interannual variability of the surface CO_2 system there (see *e.g.*, Landschützer et al. (2014) for pCO_2 variability). In the North Pacific subtropical permanently stratified (NP-STPS) biome the pH trend of -0.0016±0.0002 yr^{-1} is the same as that observed at the Hawaii Ocean Time-series (HOT, Bates et al., 2014). The trends in the two equatorial Pacific Ocean biomes differ substantially. While the western biome (WP-EQU) has a relatively weak trend (-0.0010±0.0002 yr^{-1}), the eastern (EP-EQU) biome has a much stronger pH trend than any other biome except the IO-STPS. This could be related to the recent trend toward stronger and more prevalent La Niña conditions in the eastern tropical Pacific leading to stronger upwelling, and higher surface fCO_2 and lower pH in this region (Rödenbeck et al., 2014).

The Indian Ocean subtropical permanently stratified (IO-STPS) biome had a very strong pH trend the past 30 years, only rivaled by that in the EP-EQU biome, as mentioned above. There are not any time series stations in the Indian Ocean to compare with, but fCO_2 trends for the Indian Ocean computed by Metzl (2009) are considerably larger than what we find: 2.11 μatm yr^{-1} vs 1.44±0.24 μatm yr^{-1}. Hence there is no reason to believe that our approach overestimates the pH trends here. It should be noted though that the trend identified by Metzl (2009) is based on data in a considerably smaller region than the IO-STPS which could account for some of the difference. In the Southern Ocean only the subpolar seasonally stratified (SO-SPSS) biome has a statistically significant pH trend, which at -0.0020±0.0002

291 yr^{-1} is comparable to that in the NA-SPSS biome. Furthermore, this trend is very similar to
292 that calculated for this region by Takahashi et al. (2014), although they used a different
293 method.

294 ### 3.2. Effects of changes in carbonate chemistry

295 To first order, the pH trends are expected to represent the direct response to increasing
296 oceanic DIC, as is the case for the long-term trends in surface ocean fCO_2. In order to assess
297 how our results compare with this expectation, we have calculated two expected pH rates of
298 change: first the 1981-2011 change in pH resulting from a surface ocean fCO_2 rate of change
299 equal to that in the atmosphere (1.8±0.1 μatm yr^{-1}) while keeping all other variables constant
300 at their 1981 values; and second the change in pH that would be expected if the pH change
301 mirrored the observed fCO_2 change in each biome provided that all other variables were kept
302 at their 1981 values. The first expected pH change reflects how pH should change if the
303 change in atmospheric CO_2 was the sole driver for the change in ocean pH. The second
304 expected pH change reflects how pH should change if the oceanic fCO_2 changes were allowed
305 to depart from the atmospheric ones but fCO_2 change remaining the only driver of pH change.
306 Fig. 6 shows both expected pH changes along with the observed pH change in each
307 biome. Only the 13 biomes that have statistically significant pH trends for either 1981-2011
308 or 1991-2011 (Fig. 1) are discussed further. When the atmospheric CO_2 increase is assumed
309 to be the only driver for the pH changes, we find that in 7 of the 13 biomes the observed pH
310 trends significantly differ from the expected pH change. This is due either to the uncertainty
311 in the observed trends, to associated changes in the CO_2 chemistry, or to the surface ocean
312 fCO_2 trends being significantly different from that in the atmosphere. However, the observed
313 pH trends also significantly differ from the expected pH change calculated using the observed
314 fCO_2 trend in 6 of the 13 biomes (Fig. 6). Only 3 of the biomes are the same in both cases.
315 Thus, the surface ocean fCO_2 trend not exactly mirroring the atmospheric cannot explain the
316 discrepancy between expected and observed pH trends in most biomes. It may be an
317 explanation in the equatorial Pacific biomes (EP-EQU and WP-EQU) where there is no
318 discrepancy between observed and expected pH trends when the observed fCO_2 trend is used
319 to calculate the expected pH change (Fig. 6), but a significant difference when an atmospheric
320 rate of change is assumed.
321 The observed pH trend is more often smaller than that expected for the ocean
322 mirroring the atmospheric fCO_2 change than vice versa. Only the EP-EQU and IO-STPS

biomes have observed pH changes larger than those expected (Fig. 6). Our hypothesis is that the differences between the observed and expected pH trends are caused by changes in the spatial variations in the ratio of DIC to alkalinity, which leads to spatial changes in the buffer (Revelle) factor. In the biomes where the observed trend differs from the expected trend there are indications which point to such changes. When the difference is negative (*i.e.*, the observed trend is smaller than the expected), the decrease in Revelle factor, *e.g.*, is stronger the larger the difference. However, given the combined calculation errors, generally high level of noise in our data, and relatively few data points, only some of these indications are statistically significant. Further analysis of these spatial patterns needs to be undertaken using independent pH data, preferably direct measurements in order to quantify any possible biases in the results due to our pH being a calculated variable. A combination of SOCAT data with repeat hydrography and time-series data would be ideal but this is outside the scope of this study.

3.3. Major driving forces behind the observed pH and trends

The decomposition of the fCO_2 and pH trends confirms (Figs. 7-9) that in all biomes the long-term increase in DIC is by far the dominant driver for the long-term pH changes. Knowledge about the changes in ocean DIC therefore is the most important in understanding—and predicting—changes in ocean pH (Table 2). This is not unexpected since the open ocean is in—or very close to—chemical equilibrium with the atmosphere (Lauvset and Gruber, 2014). Thus the surface ocean is taking up CO_2 from the atmosphere in order to re-establish a chemical equilibrium, leading to a corresponding increase in fCO_2 and DIC. It must be noted that since we do not have measurements of alkalinity this parameter is calculated from SST and SSS, and the relatively large uncertainties in these calculations may add a degree of uncertainty to the decomposition. Due to a lack of independent data this is not further evaluated in this study.

In the Atlantic Ocean biomes the second most important driver is SST (Fig. 7), which mostly has a positive change and therefore has limited the DIC increase required to maintain an fCO_2 growth rate similar to that in the atmosphere. SST is the second most important driver also in the Pacific Ocean biomes (except in the NP-SPSS, Fig. 8), but here SST decreased in many biomes leading to an enhanced increase in DIC through CO_2 uptake from the atmosphere. In the Southern Ocean biomes alkalinity changes have a significant impact on the trends (Fig. 9), which also modulates the DIC changes. Decreasing alkalinity over time

increases fCO_2 so that the DIC change required to maintain a sea surface fCO_2 growth rate similar to the atmospheric is reduced.

In most biomes there is a residual between the sum of the four components and the observed trend (Fig. 10). Lenton et al. (2012) performed a similar analysis and attributed such residuals to the use of a spatial mean Revelle factor, the approximations underlying the Takahashi et al. (1993) equations, and the assumption of linear trends in all variables. We tested whether variable data coverage is also an important contributor to this residual by subsampling the NorESM1-ME simulated pH data and comparing the resulting 1981-2011 decomposition with the decomposition determined using the full model output. Fig. 10 illustrates that in most biomes there are similar residuals between the sum of the four components and the actual trends in the sub-sampled and fully-sampled model fields as well. We can, therefore, find no evidence to show that poor data coverage is of major importance in determining what drives the change in surface ocean pH.

3.4. Recent changes in the Southern Ocean biomes

In contrast to the majority of the global ocean biomes, trends within the SO-STSS and SO-ICE biomes do not appear statistically significant over the past two decades (Table 1). This can be linked to strong interannual and decadal variations (Fig. 3). This is consistent with the changing fCO_2 trends revealed in a recent study by Fay et al. (2014) as well as previous findings of a change in the CO_2 sink in this region (*e.g.* Fay and McKinley, 2013; Landschützer et al., 2014). In order to investigate these recent changes in the trend in the Southern Ocean, we also decompose the 2001-2011 trends in the Southern Ocean biomes (Table 3).

In the SO-STSS biome there is no significant change in pH over the 30 year period, but from Fig. 3 it is seen that there is a decrease until ~2000 and then an increase over the last decade. Over the last decade (Table 3) we find that the contributions of the individual parameters to the overall trend in pH are amplified. Temperature and DIC changes remain the strongest drivers, and of these the forcing from DIC has increased strongest over the last decade. We hence conclude that the increase in pH over the past decade in the SO-STSS biome is due to the decreasing DIC concentrations dominating over the thermally induced reduction in pH.

In the SO-SPSS biome the pH trend appears to become less steep over the last decade (Fig. 3), which is consistent with the well-documented trend changes in fCO_2. In this biome

we find a less negative DIC driven pH trend in the period 2001-2011 compared to the period 1981-2011, indicating a reduced increasing trend in DIC over this decade. This supports the conclusion drawn by Fay and McKinley (2013) that a reduction in vertical DIC supply causes a weakening of both fCO_2 and pH trends in this region. In the SO-ICE biome the sign of the non-thermal drivers appears to change within the last decade, potentially driven by the recent Antarctic ice melt and ice-sheet melting driven iron fertilization (Death et al., 2014).

3.5. Spatial variability

In both the observations and the sub-sampled model results we see significant regional differences in the pH trends (Fig. 5). Note that the actual simulated pH trends in each biome are not directly comparable with the observed trends since the model is a coupled climate model, which simulates its own internal climate variability. We therefore compare the fully sampled and the sub-sampled model results, and the fully sampled model results show much more uniform pH trends (Fig. 5). While these differences are mostly statistically indistinguishable within the uncertainties, it highlights the need for careful consideration of representativeness when comparing model-derived future changes and trends based on data. Fig. 5 shows that in the IO-STPS and WP-EQU biomes the sub-sampled trend is within ±0.0001 of the fully-sampled pH trends, and an ANOVA analysis shows that only in the SP-STPS biome are the two model trends significantly different. Thus the trends based on the existing observational coverage are overall representative of the respective biomes, and it is unlikely that there are major biases in our results due to low data density. However, the uncertainties in the long-term pH trend estimates remain large, both in observations and the model (Fig. 5) and this prohibits a mechanistic understanding the observed changes in most biomes. Improved sampling strategies are necessary to reduce these uncertainties and thereby improve our understanding of surface ocean CO_2 chemistry changes today and in the future.

This highlights the importance of both maintaining the observational networks already in place—like the voluntary observing ship (VOS) network in the North Atlantic (Watson et al., 2009)—and instigating new ones in less well-covered ocean regions. Of particular importance is improved data coverage in the Southern Pacific Ocean (SP-STPS) where the data density as of today it too low for a robust analysis of long term pH trends.

4. Conclusions

Global surface ocean pH changes over the past 30 years cannot be calculated as there are too few data in many biomes. For the past twenty years on the other hand, we find that the surface ocean pH has decreased by on average 0.0018±0.0004 yr^{-1}, excluding the Arctic and high-latitude Southern Ocean. There are however large regional variations with trends ranging from -0.0024 yr^{-1} in the Indian Ocean (IO-STPS) biome to no significant change in the polar Southern Ocean (SO-ICE) biome. Our estimated global trend is comparable to the trends found at time-series stations and to the global average trend in the NorESM1-ME model. In all biomes, the pH trend is predominantly driven by changes in DIC, implying that the surface ocean pH decline is a direct response to the increasing uptake of atmospheric CO_2. Despite this, the fCO_2 and pH trends do not exactly mirror each other, which is potentially linked to trends in the surface ocean buffer (Revelle) factor over the past decades. In some biomes this leads to smaller pH changes than expected from the fCO_2 change, while in others regions, the pH changes are larger than expected. Thus, knowledge of both the changing ocean DIC and the changing ocean buffer (Revelle) factor is important for understanding and accurately determining the changing ocean pH.

There are regional differences in the pH trends. It is likely that these are caused by spatial heterogeneity in the concurrent changes in buffer (Revelle) factor, while spatial heterogeneity in the surface ocean fCO_2 trends seems to have only a minor effect. Our comparison between fully-sampled model and sub-sampled output from the NorESM1-ME model indicates that variable data coverage only presents a major problem in the South Pacific. This nicely highlights the overall success of the scientific community in creating observational networks that reduce data coverage issues. The many scientific studies arising from this effort—among many others the recent publications by Nakaoka et al. (2013), Landschützer et al. (2013), Landschützer et al. (2014), and Schuster et al. (2013)—show that we have come a long way in understanding how ocean CO_2 chemistry is evolving in a world perturbed by fossil fuel emissions. The uncertainties in the trends presented here are, however, substantial and this largely prevents a more thorough understanding of current changes. Filling the remaining gaps in our surface ocean data is, therefore, still of great importance.

Acknowledgements

The work of S. K. Lauvset was funded by the Norwegian Reseach Council through the project DECApH (214513/F20). Are Olsen acknowledge funding from the Centre for Climate Dynamics at the Bjerknes Centre for Climate Research, and the Norwegian Research Councul project SNACS (229756). N. Gruber and P. Landschützer acknowledge funding from the ETH and the EU FP7 projects CARBOCHANGE (264879) and GEOCARBON (283080). J. Tjiputra acknowledges the Centre for Climate Dynamics project BIOFEEDBACK.

References

Antonov, J., Seidov, D., Boyer, T., Locarnini, R., Mishonov, A., Garcia, H., Baranova, O., Zweng, M., and Johnson, D.: World Ocean Atlas 2009, vol. 2, Salinity, edited by S. Levitus, 184 pp, US Gov. Print. Off., Washington, DC, 2010. 2010.

Bakker, D. C. E., Pfeil, B., Smith, K., Hankin, S., Olsen, A., Alin, S. R., Cosca, C., Harasawa, S., Kozyr, A., Nojiri, Y., O'Brien, K. M., Schuster, U., Telszewski, M., Tilbrook, B., Wada, C., Akl, J., Barbero, L., Bates, N. R., Boutin, J., Bozec, Y., Cai, W. J., Castle, R. D., Chavez, F. P., Chen, L., Chierici, M., Currie, K., de Baar, H. J. W., Evans, W., Feely, R. A., Fransson, A., Gao, Z., Hales, B., Hardman-Mountford, N. J., Hoppema, M., Huang, W. J., Hunt, C. W., Huss, B., Ichikawa, T., Johannessen, T., Jones, E. M., Jones, S. D., Jutterström, S., Kitidis, V., Körtzinger, A., Landschützer, P., Lauvset, S. K., Lefèvre, N., Manke, A. B., Mathis, J. T., Merlivat, L., Metzl, N., Murata, A., Newberger, T., Omar, A. M., Ono, T., Park, G. H., Paterson, K., Pierrot, D., Ríos, A. F., Sabine, C. L., Saito, S., Salisbury, J., Sarma, V. V. S. S., Schlitzer, R., Sieger, R., Skjelvan, I., Steinhoff, T., Sullivan, K. F., Sun, H., Sutton, A. J., Suzuki, T., Sweeney, C., Takahashi, T., Tjiputra, J., Tsurushima, N., van Heuven, S. M. A. C., Vandemark, D., Vlahos, P., Wallace, D. W. R., Wanninkhof, R., and Watson, A. J.: An update to the Surface Ocean CO2 Atlas (SOCAT version 2), Earth Syst. Sci. Data, 6, 69-90, 2014.

Bates, N. R.: Interannual variability of the oceanic CO2 sink in the subtropical gyre of the North Atlantic Ocean over the last 2 decades, J. Geophys. Res.-Oceans, 112, 26, 2007.

Bates, N. R., Astor, Y. M., Church, M. J., Currie, K., Dore, J. E., Gonzalez-Davila, M., Lorenzoni, L., Muller-Karger, F., Olafsson, J., and Magdalena Santana-Casiano, J.: A Time-Series View of Changing Surface Ocean Chemistry Due to Ocean Uptake of Anthropogenic CO2 and Ocean Acidification, Oceanography, 27, 126-141, 2014.

Bopp, L., Resplandy, L., Orr, J. C., Doney, S. C., Dunne, J. P., Gehlen, M., Halloran, P., Heinze, C., Ilyina, T., Seferian, R., Tjiputra, J., and Vichi, M.: Multiple stressors of

ocean ecosystems in the 21st century: projections with CMIP5 models, Biogeosciences, 10, 6225-6245, 2013.

Dickson, A.G. and Millero, F.J., 1987. A comparison of the equilibrium-constants for the dissociation of carbonic-acid in seawater media. Deep-Sea Research Part a-Oceanographic Research Papers, 34(10): 1733-1743.

Death, R., Wadham, J. L., Monteiro, F., Le Brocq, A. M., Tranter, M., Ridgwell, A., Dutkiewicz, S., and Raiswell, R.: Antarctic ice sheet fertilises the Southern Ocean, Biogeosciences, 11, 2635-2643, 2014.

Doney, S. C., Balch, W. M., Fabry, V. J., and Feely, R. A.: Ocean Acidification: A critical emerging problem for the ocean sciences, Oceanography, 22, 16-25, 2009a.

Doney, S. C., Fabry, V. J., Feely, R. A., and Kleypas, J. A.: Ocean Acidification: The Other CO2 Problem, Annual Review of Marine Science, 1, 169-192, 2009b.

Dore, J. E., Lukas, R., Sadler, D. W., Church, M. J., and Karl, D. M.: Physical and biogeochemical modulation of ocean acidification in the central North Pacific, Proceedings of the National Academy of Sciences, 106, 12235-12240, 2009.

Fay, A. R. and McKinley, G. A.: Global trends in surface ocean pCO_2 from in situ data, Global Biogeochemical Cycles, 27, 541-557, 2013.

Fay, A. R. and McKinley, G. A.: Global Ocean Biomes: Mean and time-varying maps (NetCDF 7.8 MB), doi:10.1594/PANGAEA.828650, 2014, Supplement to: Fay, A. R. and McKinley, G. A.: Global open-ocean biomes: mean and temporal variability, Earth Syst. Sci. Data, 6, 273–284, doi: 10.5194/essd-6-273-2014, 2014.

Fay, A. R., McKinley, G. A., and Lovenduski, N. S.: Southern Ocean carbon trends: sensitivity to methods, Geophys. Res. Lett., 41, doi: 10.1002/2014GL061324, online first, 2014.

Gattuso, J.-P. and Hansson, L.: Ocean Acidification, Oxford University Press, New York, 2011

Gonzalez-Davila, M., Santana-Casiano, J. M., and Gonzalez-Davila, E. F.: Interannual variability of the upper ocean carbon cycle in the northeast Atlantic Ocean, Geophysical Research Letters, 34, 2007.

Gonzalez-Davila, M., Santana-Casiano, J. M., Rueda, M. J., and Llinas, O.: The water column distribution of carbonate system variables at the ESTOC site from 1995 to 2004, Biogeosciences, 7, 3067-3081, 2010.

514 Landschützer, P., Gruber, N., Bakker, D. C. E., and Schuster, U.: Recent variability of the
515 global ocean carbon sink, Global Biogeochemical Cycles, doi: 10.1002/2014GB004853,
516 2014. 2014GB004853, 2014.
517 Landschützer, P., Gruber, N., Bakker, D. C. E., Schuster, U., Nakaoka, S., Payne, M. R.,
518 Sasse, T. P., and Zeng, J.: A neural network-based estimate of the seasonal to inter-
519 annual variability of the Atlantic Ocean carbon sink, Biogeosciences, 10, 7793-7815,
520 2013.
521 Lauvset, S. K. and Gruber, N.: Long-term trends in surface ocean pH in the North Atlantic,
522 Marine Chemistry, 162, 71-76, 2014.
523 Lewis, E. and Wallace, D.W.R.: Program developed for CO2 system calculations,
524 ORNL/CDIAC-105. Carbon Dioxide Information Analysis Center, Oak Ridge National
525 Laboratory, U.S. Department of Energy, Oak Ridge, Tennessee, 1998.
526 Le Quéré, C.: Trends in the land and ocean carbon uptake, Current Opinion in Environmental
527 Sustainability, 2, 219-224, 2010.
528 Le Quéré, C., Peters, G. P., Andres, R. J., Andrew, R. M., Boden, T. A., Ciais, P.,
529 Friedlingstein, P., Houghton, R. A., Marland, G., Moriarty, R., Sitch, S., Tans, P.,
530 Arneth, A., Arvanitis, A., Bakker, D. C. E., Bopp, L., Canadell, J. G., Chini, L. P.,
531 Doney, S. C., Harper, A., Harris, I., House, J. I., Jain, A. K., Jones, S. D., Kato, E.,
532 Keeling, R. F., Klein Goldewijk, K., Körtzinger, A., Koven, C., Lefèvre, N., Maignan,
533 F., Omar, A., Ono, T., Park, G. H., Pfeil, B., Poulter, B., Raupach, M. R., Regnier, P.,
534 Rödenbeck, C., Saito, S., Schwinger, J., Segschneider, J., Stocker, B. D., Takahashi, T.,
535 Tilbrook, B., van Heuven, S., Viovy, N., Wanninkhof, R., Wiltshire, A., and Zaehle, S.:
536 Global carbon budget 2013, Earth Syst. Sci. Data, 6, 235-263, 2014.
537 Lee, K., Tong, L. T., Millero, F. J., Sabine, C. L., Dickson, A. G., Goyet, C., Park, G.-H.,
538 Wanninkhof, R., Feely, R. A., and Key, R. M.: Global relationships of total alkalinity
539 with salinity and temperature in surface waters of the world's oceans, Geophysical
540 Research Letters, 33, L19605, 2006.
541 Lenton, A., Metzl, N., Takahashi, T., Kuchinke, M., Matear, R. J., Roy, T., Sutherland, S. C.,
542 Sweeney, C., and Tilbrook, B.: The observed evolution of oceanic pCO2 and its drivers
543 over the last two decades, Global Biogeochem. Cycles, 26, GB2021, 2012.
544 McGrath, T., Kivimae, C., Tanhua, T., Cave, R. R., and McGovern, E.: Inorganic carbon and
545 pH levels in the Rockall Trough 1991-2010, Deep-Sea Research Part I-Oceanographic
546 Research Papers, 68, 79-91, 2012.

Mehrbach, C., Culberso.Ch, Hawley, J.E. and Pytkowic.Rm, 1973. Measurement of apparent dissociation-constants of carbonic-acid in seawater at atmospheric-pressure. Limnology and Oceanography, 18(6): 897-907.

Metzl, N.: Decadal increase of oceanic carbon dioxide in Southern Indian Ocean surface waters (1991–2007), Deep Sea Research Part II: Topical Studies in Oceanography, 56, 607-619, 2009.

Nakaoka, S., Telszewski, M., Nojiri, Y., Yasunaka, S., Miyazaki, C., Mukai, H., and Usui, N.: Estimating temporal and spatial variation of ocean surface pCO2 in the North Pacific using a self-organizing map neural network technique, Biogeosciences, 10, 6093-6106, 2013.

Nondal, G., Bellerby, R. G. J., Olsen, A., Johannessen, T., and Olafsson, J.: Optimal evaluation of the surface ocean CO2 system in the northern North Atlantic using data from voluntary observing ships, Limnol. Oceanogr. Meth., 7, 109-118, 2009.

Olafsson, J., Olafsdottir, S. R., Benoit-Cattin, A., and Takahashi, T.: The Irminger Sea and the Iceland Sea time series measurements of sea water carbon and nutrient chemistry 1983–2008, Earth Syst. Sci. Data, 2, 99-104, 2010.

Orr, J.: Recent and future changes in ocean carbonate chemistry. In: Ocean acidification, Gattuso, J.-P. and Hansson, L. (Eds.), Oxford University Press, New York, 41-66, 2011.

Pfeil, B., Olsen, A., Bakker, D. C. E., Hankin, S., Koyuk, H., Kozyr, A., Malczyk, J., Manke, A., Metzl, N., Sabine, C. L., Akl, J., Alin, S. R., Bates, N., Bellerby, R. G. J., Borges, A., Boutin, J., Brown, P. J., Cai, W. J., Chavez, F. P., Chen, A., Cosca, C., Fassbender, A. J., Feely, R. A., González-Dávila, M., Goyet, C., Hales, B., Hardman-Mountford, N., Heinze, C., Hood, M., Hoppema, M., Hunt, C. W., Hydes, D., Ishii, M., Johannessen, T., Jones, S. D., Key, R. M., Körtzinger, A., Landschützer, P., Lauvset, S. K., Lefèvre, N., Lenton, A., Lourantou, A., Merlivat, L., Midorikawa, T., Mintrop, L., Miyazaki, C., Murata, A., Nakadate, A., Nakano, Y., Nakaoka, S., Nojiri, Y., Omar, A. M., Padin, X. A., Park, G. H., Paterson, K., Perez, F. F., Pierrot, D., Poisson, A., Ríos, A. F., Santana-Casiano, J. M., Salisbury, J., Sarma, V. V. S. S., Schlitzer, R., Schneider, B., Schuster, U., Sieger, R., Skjelvan, I., Steinhoff, T., Suzuki, T., Takahashi, T., Tedesco, K., Telszewski, M., Thomas, H., Tilbrook, B., Tjiputra, J., Vandemark, D., Veness, T., Wanninkhof, R., Watson, A. J., Weiss, R., Wong, C. S., and Yoshikawa-Inoue, H.: A uniform, quality controlled Surface Ocean CO2 Atlas (SOCAT), Earth Syst. Sci. Data, 5, 125-143, 2013.

Rödenbeck, C., Bakker, D. C. E., Metzl, N., Olsen, A., Sabine, C., Cassar, N., Reum, F., Keeling, R. F., and Heimann, M.: Interannual sea–air CO_2 flux variability from an observation-driven ocean mixed-layer scheme, Biogeosciences, 11, 4599–4613, doi:10.5194/bg-11-4599-2014, 2014.

Sarmiento, J. L. and Gruber, N.: Ocean biogeochemical dynamics, Princeton University Press, Princeton, N.J., 2006.

Schuster, U., McKinley, G. A., Bates, N., Chevallier, F., Doney, S. C., Fay, A. R., González-Dávila, M., Gruber, N., Jones, S., Krijnen, J., Landschützer, P., Lefèvre, N., Manizza, M., Mathis, J., Metzl, N., Olsen, A., Rios, A. F., Rödenbeck, C., Santana-Casiano, J. M., Takahashi, T., Wanninkhof, R., and Watson, A. J.: An assessment of the Atlantic and Arctic sea–air CO2 fluxes, 1990–2009, Biogeosciences, 10, 607-627, 2013.

Steinacher, M., Joos, F., Froelicher, T. L., Plattner, G. K., and Doney, S. C.: Imminent ocean acidification in the Arctic projected with the NCAR global coupled carbon cycle-climate model, Biogeosciences, 6, 515-533, 2009.

Takahashi, T., Olafsson, J., Goddard, J. G., Chipman, D. W., and Sutherland, S. C.: Seasonal-Variation of CO2 and Nutrients in the High-Latitude Surface Oceans - A Comparative Study, Global Biogeochemical Cycles, 7, 843-878, 1993.

Takahashi, T., Sutherland, S. C., Chipman, D. W., Goddard, J. G., Ho, C., Newberger, T., Sweeney, C., and Munro, D. R.: Climatological distributions of pH, pCO2, total CO2, alkalinity, and CaCO3 saturation in the global surface ocean, and temporal changes at selected locations, Marine Chemistry, 164, 95-125, 2014.

Takahashi, T., Sutherland, S. C., and Kozyr, A.: Global Ocean Surface Water Partial Pressure of CO2 Database: Measurements Performed During 1968-2008 (Version 2008). . In: ORNL/CDIAC-152, NDP-088r, Carbon Dioxide Information Analysis Center, Oak Ridge National Laboratory, U.S. Department of Energy, Oak Ridge, Tennessee, 2009a.

Takahashi, T., Sutherland, S. C., Sweeney, C., Poisson, A., Metzl, N., Tilbrook, B., Bates, N. R., Wanninkhof, R., Feely, R. A., Sabine, C. L., Olafsson, J., and Nojiri, Y.: Global sea-air CO2 flux based on climatological surface ocean pCO2, and seasonal biological and temperature effects, Deep-Sea Research II, 49, 1601-1622, 2002.

Takahashi, T., Sutherland, S. C., Wanninkhof, R., Sweeney, C., Feely, R. A., Chipman, D. W., Hales, B., Friederich, G., Chavez, F., Sabine, C., Watson, A., Bakker, D. C. E., Schuster, U., Metzl, N., Yoshikawa-Inoue, H., Ishii, M., Midorikawa, T., Nojiri, Y., Körtzinger, A., Steinhoff, T., Hoppema, M., Olafsson, J., Arnarson, T. S., Tilbrook, B.,

Johannessen, T., Olsen, A., Bellerby, R., Wong, C. S., Delille, B., Bates, N. R., and de Baar, H. J. W.: Climatological mean and decadal change in surface ocean pCO2, and net sea-air CO2 flux over the global oceans, Deep-Sea Research Part II - Topical Studies in Oceanography, 56, 554-577, 2009b.

Taylor, K. E., Stouffer, R. J., and Meehl, G. A.: AN OVERVIEW OF CMIP5 AND THE EXPERIMENT DESIGN, Bulletin of the American Meteorological Society, 93, 485-498, 2012.

Tjiputra, J. F., Olsen, A. R. E., Bopp, L., Lenton, A., Pfeil, B., Roy, T., Segschneider, J., Totterdell, I. A. N., and Heinze, C.: Long-term surface pCO2trends from observations and models, Tellus B, 66, 2014.

Tjiputra, J. F., Roelandt, C., Bentsen, M., Lawrence, D. M., Lorentzen, T., Schwinger, J., Seland, O., and Heinze, C.: Evaluation of the carbon cycle components in the Norwegian Earth System Model (NorESM), Geoscientific Model Development, 6, 301-325, 2013.

Uppstrom, L.R., 1974. BORON/CHLORINITY RATIO OF DEEP-SEA WATER FROM PACIFIC OCEAN. Deep-Sea Research, 21(2): 161-162.

Vijayvargiya, A.: One-Way Analysis of Variance, Journal of Validation Technology, 15, 62-63, 2009.

Watson, A. J., Schuster, U., Bakker, D. C. E., Bates, N. R., Corbiere, A., Gonzalez-Davila, M., Friedrich, T., Hauck, J., Heinze, C., Johannessen, T., Körtzinger, A., Metzl, N., Olafsson, J., Olsen, A., Oschlies, A., Padin, X. A., Pfeil, B., Santana-Casiano, J. M., Steinhoff, T., Telszewski, M., Rios, A. F., Wallace, D. W. R., and Wanninkhof, R.: Tracking the Variable North Atlantic Sink for Atmospheric CO2, Science, 326, 1391-1393, 2009.

Zeebe, R., E. and Wolf-Gladrow, D.: CO2 in seawater, equilibrium, kinetics, isotopes, Elsevier, Amsterdam, PAYS-BAS, 2001.

Table 1. Results and statistics of the regression analysis of fCO_2 (µatm) and pH_{insitu} versus time. Bold text indicates biomes where the results are not statistically significant (95% confidence). No number is given if a biome does not have enough data to calculate the trend in a given time period.

	1981 – 2011				1991 – 2011			
	pH		fCO_2		pH		fCO_2	
region	slope	rmse	slope	rmse	slope	rmse	slope	rmse
NP-SPSS	**-0.0003±0.0005**	**0.041**	1.20±0.17	16.2	0.0013±0.0005	0.038	0.74±0.22	16.1
NP-STSS	---	---	1.30±0.15	10.5	-0.0010±0.0005	0.031	1.37±0.13	8.9
NP-STPS	-0.0016±0.0002	0.020	1.51±0.09	10.3	-0.0019±0.0002	0.018	1.52±0.12	9.9
WP-EQU	-0.0010±0.0002	0.016	1.54±0.19	17.8	-0.0012±0.0002	0.015	1.59±0.27	17.3
EP-EQU	-0.0023±0.0003	0.023	2.94±0.41	28.2	-0.0026±0.0002	0.023	3.51±0.51	27.9
SP-STPS	-0.0019±0.0002	0.020	1.34±0.11	12.0	-0.0022±0.0003	0.020	1.12±0.18	12.3
NA-SPSS	---	---	1.18±0.22	15.4	-0.0020±0.0004	0.028	1.11±0.22	14.2
NA-STSS	---	---	1.78±0.20	12.3	-0.0018±0.0003	0.015	1.79±0.20	12.5
NA-STPS	---	---	1.42±0.12	8.5	-0.0011±0.0002	0.012	1.44±0.12	8.6
A-EQU	---	---	1.86±0.35	16.6	-0.0016±0.0003	0.014	1.81±0.32	15.7
SA-STPS	---	---	1.06±0.37	16.7	-0.0011±0.0005	0.024	0.99±0.37	17.0
IO-STPS	-0.0024±0.0004	0.023	1.49±0.25	13.6	-0.0027±0.0005	0.025	1.55±0.26	13.5
SO-STSS	**-0.0006±0.0004**	**0.032**	1.78±0.11	10.8	**-0.0004±0.0004**	**0.032**	1.82±0.12	10.8
SO-SPSS	-0.0020±0.0002	0.020	1.44±0.10	9.1	-0.0021±0.0002	0.020	1.46±0.11	9.0
SO-ICE	---	---	0.34±0.31	24.4	**-0.0002±0.0004**	**0.029**	0.23±0.34	24.3

Table 2. Decomposition of the fCO_2 and pH_{insitu} trends into their major drivers. The units are μatm yr^{-1} and pH-units yr^{-1} respectively.

Region	pH					fCO_2				
	theta	salinity	DIC	alkalinity	sum	theta	salinity	DIC	alkalinity	sum
NP-SPSS	-0.57	-0.15	3.18	-3.04	-0.58	0.52	0.14	-2.89	2.76	0.53
NP-STSS	-0.39	0.02	-0.89	-0.13	-1.39	0.38	-0.02	0.87	0.13	1.37
NP-STPS	1.15	-0.02	-1.68	0.04	-0.50	-1.19	0.02	1.73	-0.05	0.51
WP-EQU	-0.47	0.11	-0.87	0.14	-1.10	0.53	-0.12	0.97	-0.15	1.23
EP-EQU	0.51	-0.07	-2.99	0.13	-2.42	-0.63	0.08	3.68	-0.15	2.99
SP-STPS	2.28	-0.11	-3.02	0.04	-0.81	-2.47	0.12	3.28	-0.05	0.88
NA-SPSS	-0.02	0.17	-2.41	0.12	-2.13	0.01	-0.16	2.17	-0.11	1.91
NA-STSS	0.74	-0.07	-1.43	-0.11	-0.87	-0.72	0.07	1.40	0.10	0.85
NA-STPS	-1.20	-0.05	-0.10	-0.12	-1.47	1.29	0.05	0.11	0.13	1.57
A-EQU	-0.21	0.02	-1.33	-0.05	-1.56	0.24	-0.03	1.53	0.06	1.80
SA-STPS	-0.31	0.06	-1.55	-0.05	-1.85	0.34	-0.07	1.69	0.05	2.02
IO-STPS	0.80	-0.02	-3.23	0.06	-2.39	-0.79	0.02	3.22	-0.06	2.38
SO-STSS	-0.99	-0.08	2.02	-0.86	0.09	0.88	0.08	-1.81	0.77	-0.08
SO-SPSS	0.89	0.01	-3.09	0.53	-1.66	-0.83	-0.01	2.89	-0.50	1.56
SO-ICE	0.13	-0.01	-2.22	0.15	-1.95	-0.12	0.01	2.02	-0.13	1.78

Table 3. Decomposition of the 2001-2011 fCO_2 and pH_{insitu} trends in the Southern Ocean into their major drivers. The units are μatm yr^{-1} and pH-units yr^{-1} respectively.

Region	pH						fCO_2					
	theta	salinity	DIC	alkalinity	sum	observed	theta	salinity	DIC	alkalinity	sum	observed
SO-STSS	-3.7	-0.79	8.46	-2.48	1.49	0.0032±0.0010	3.4	0.73	-7.78	2.28	-1.37	1.56±0.39
SO-SPSS	1.11	-0.07	-1.28	-0.05	-0.29	-0.0011±0.0006	-1.06	0.07	1.22	0.05	0.28	0.89±0.22
SO-ICE	-0.62	-0.05	1	-0.39	-0.06	0.0006±0.0009	0.59	0.05	-0.95	0.37	0.06	0.21±0.74

Fig. 1. A map of the Fay and McKinley (2014) biomes which have (a) a statistically significant pH trend in the period 1981-2011, and (b) the biomes with a statistically significant pH trend in the period 1991-2011.

Fig. 2. Long term pH trend (1981-2011) in the five Atlantic Ocean biomes.

Fig. 3. Long term pH trend (1981-2011) in the five Pacific Ocean biomes.

Fig. 4. Long term pH trend (1981-2011) in the Indian Ocean biome and the three Southern Ocean biomes.

Fig. 5. Summary of the pH trends in all biomes. The error bars show the 1σ confidence interval.

Fig. 6. Comparison between the observed pH trend in each biome (either 1981-2011 or 1991-2011) in black and the pH trends expected if the surface ocean fCO_2 changed equal to the atmosphere (blue) and expected for the observed ocean fCO_2 trends (red).

Fig. 7. The long term trends in pH from Fig. 2 decomposed into the contributions from SST, SSS, alkalinity, and DIC. Also shown is the sum of the four contributions and the actual observed trend. Note that the trend has been multiplied by 1000 for easier visualization.

Fig. 8. The long term trends in pH from Fig. 3 decomposed into the contributions from SST, SSS, alkalinity, and DIC. Also shown is the sum of the four contributions and the actual observed trend. Note that the trend has been multiplied by 1000 for easier visualization.

Fig. 9. The long term trends in pH from Fig. 4 decomposed into the contributions from SST, SSS, alkalinity, and DIC. Also shown is the sum of the four contributions and the actual observed trend. Note that the trend has been multiplied by 1000 for easier visualization.

Fig. 10. The residual between the actual pH trends and the sum of the four decomposition parts (SSS, SST, DIC, ALK). In gray is the residual for the observations, in black the residual for the sub-sampled model output, and in white the residual for the fully-sampled model output.

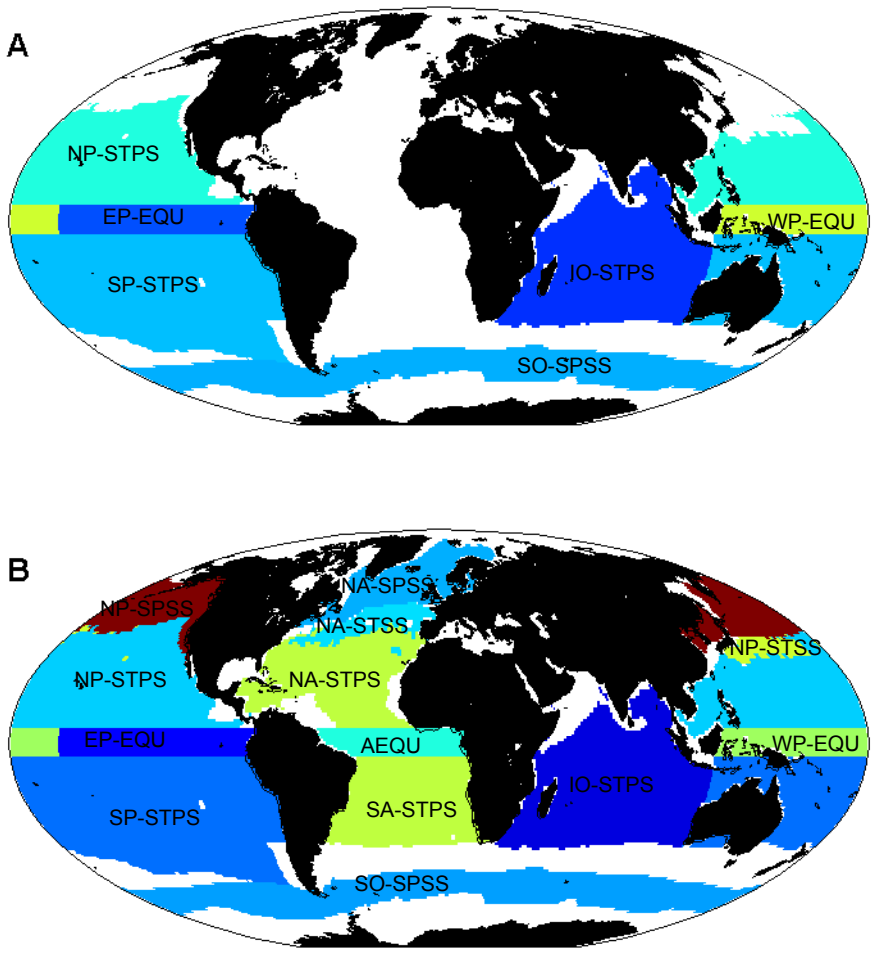
A
NP-STPS
EP-EQU
WP-EQU
SP-STPS
IO-STPS
SO-SPSS
B
NA-SPSS
NP-SPSS
NA-STSS
NP-STSS
NP-STPS
NA-STPS
EP-EQU
AEQU
WP-EQU
IO-STPS
SP-STPS
SA-STPS
SO-SPSS
-3
-2.5
-2
-1.5
-1
-0.5
0
0.5
x 10^-3

Figure 1

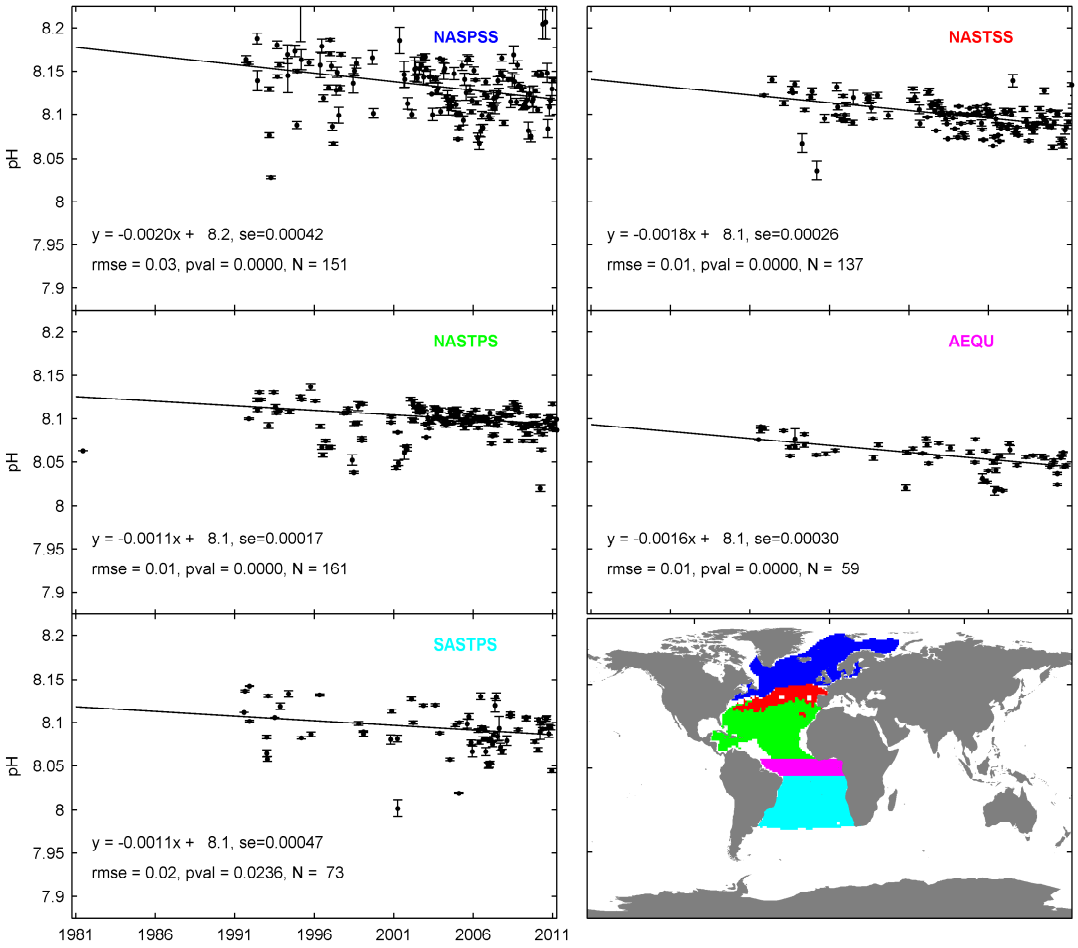
NASPSS
y = -0.0020x + 8.2, se=0.00042
rmse = 0.03, pval = 0.0000, N = 151
NASTSS
y = -0.0018x + 8.1, se=0.00026
rmse = 0.01, pval = 0.0000, N = 137
NASTPS
y = -0.0011x + 8.1, se=0.00017
rmse = 0.01, pval = 0.0000, N = 161
AEQU
y = -0.0016x + 8.1, se=0.00030
rmse = 0.01, pval = 0.0000, N = 59
SASTPS
y = -0.0011x + 8.1, se=0.00047
rmse = 0.02, pval = 0.0236, N = 73
pH
8.2
8.15
8.1
8.05
8
7.95
7.9
1981
1986
1991
1996
2001
2006
2011

Figure 2

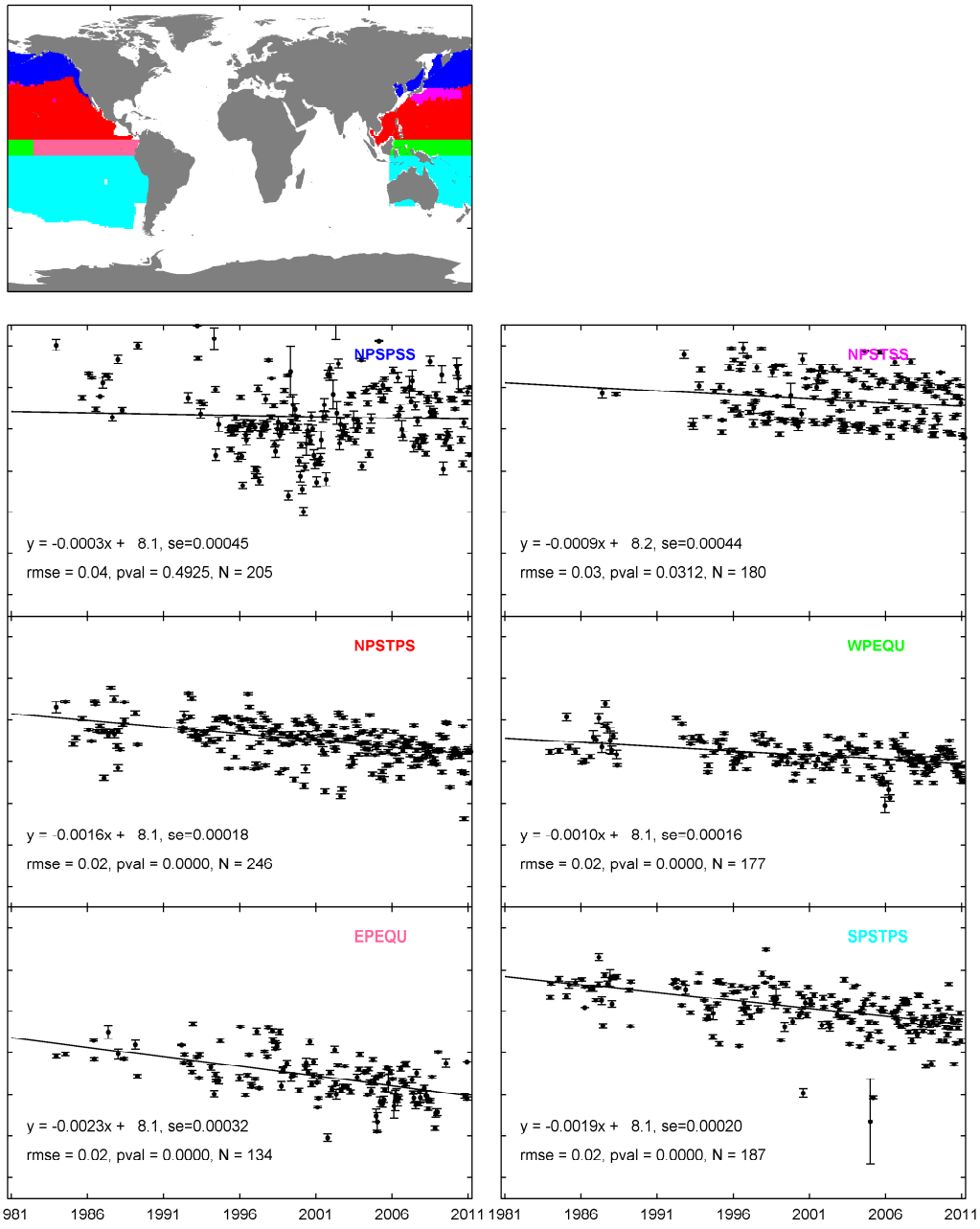
NPSPSS
y = -0.0003x + 8.1, se=0.00045
rmse = 0.04, pval = 0.4925, N = 205
NPSTSS
y = -0.0009x + 8.2, se=0.00044
rmse = 0.03, pval = 0.0312, N = 180
NPSTPS
y = -0.0016x + 8.1, se=0.00018
rmse = 0.02, pval = 0.0000, N = 246
WPEQU
y = -0.0010x + 8.1, se=0.00016
rmse = 0.02, pval = 0.0000, N = 177
EPEQU
y = -0.0023x + 8.1, se=0.00032
rmse = 0.02, pval = 0.0000, N = 134
SPSTPS
y = -0.0019x + 8.1, se=0.00020
rmse = 0.02, pval = 0.0000, N = 187
pH
8.2
8.15
8.1
8.05
8
7.95
7.9
1981
1986
1991
1996
2001
2006
2011

Figure 3

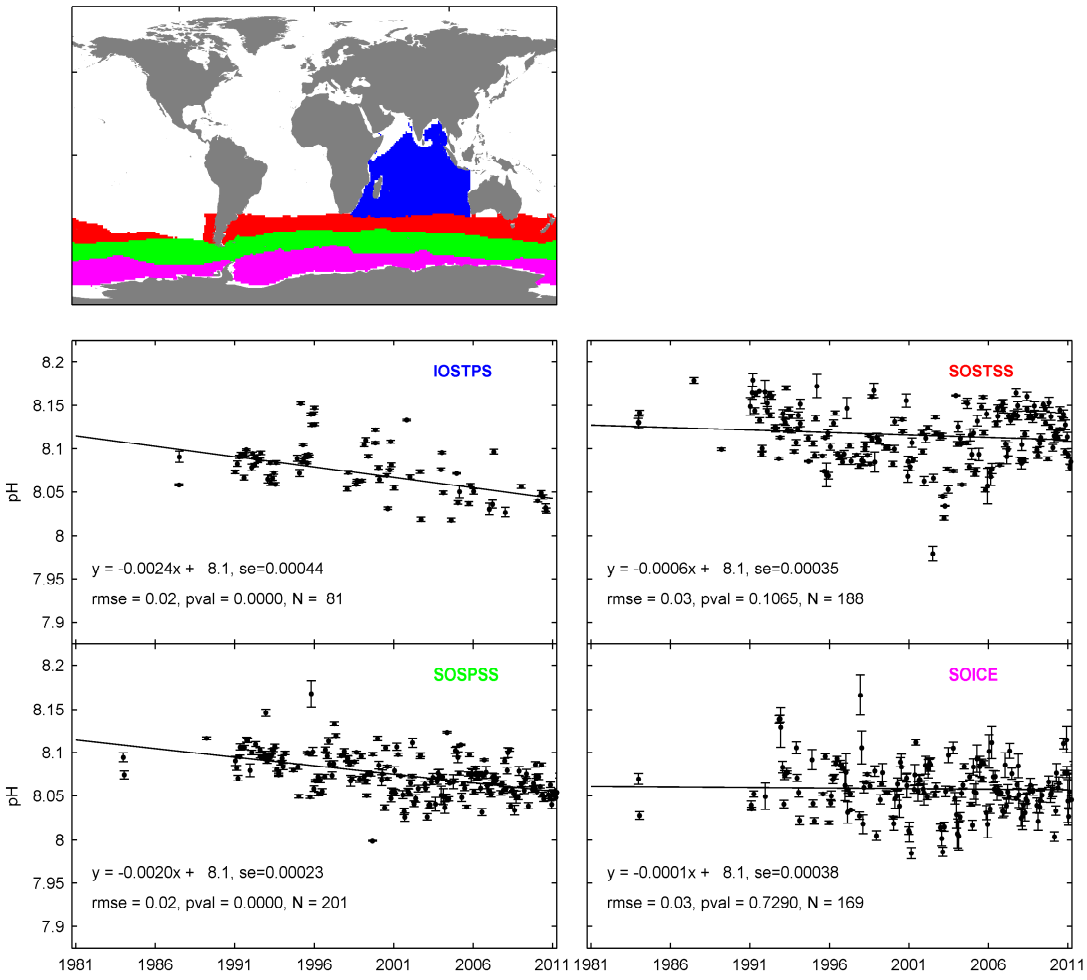
IOSTPS
y = -0.0024x + 8.1, se=0.00044
rmse = 0.02, pval = 0.0000, N = 81
SOSTSS
y = -0.0006x + 8.1, se=0.00035
rmse = 0.03, pval = 0.1065, N = 186
SOSPSS
y = -0.0020x + 8.1, se=0.00023
rmse = 0.02, pval = 0.0000, N = 201
SOICE
y = -0.0001x + 8.1, se=0.00038
rmse = 0.03, pval = 0.7290, N = 169
pH
8.2
8.15
8.1
8.05
8
7.95
7.9
1981
1986
1991
1996
2001
2006
2011

Figure 4

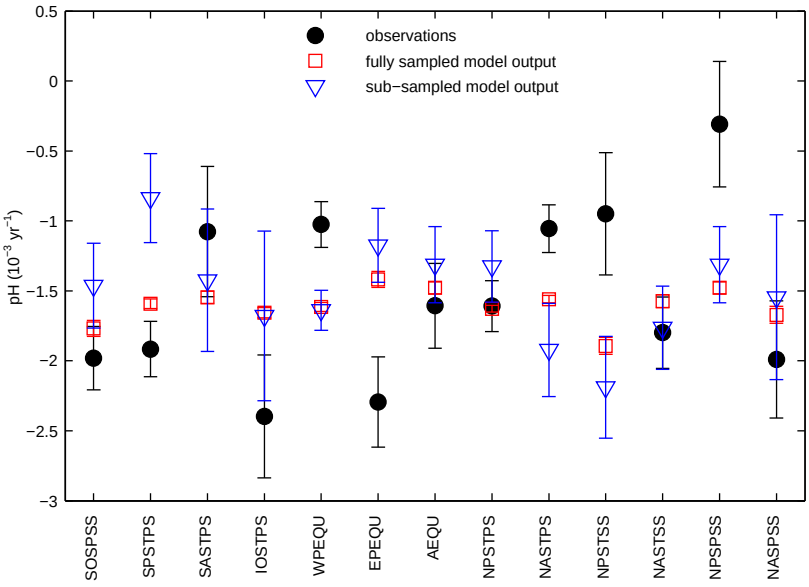
observations
fully sampled model output
sub−sampled model output
pH (10^{-3} yr^{-1})
0.5
0
−0.5
−1
−1.5
−2
−2.5
−3
SOSPSS
SPSTPS
SASTPS
IOSTPS
WPEQU
EPEQU
AEQU
NPSTPS
NASTPS
NPSTSS
NASTSS
NPSPSS
NASPSS

Figure 5

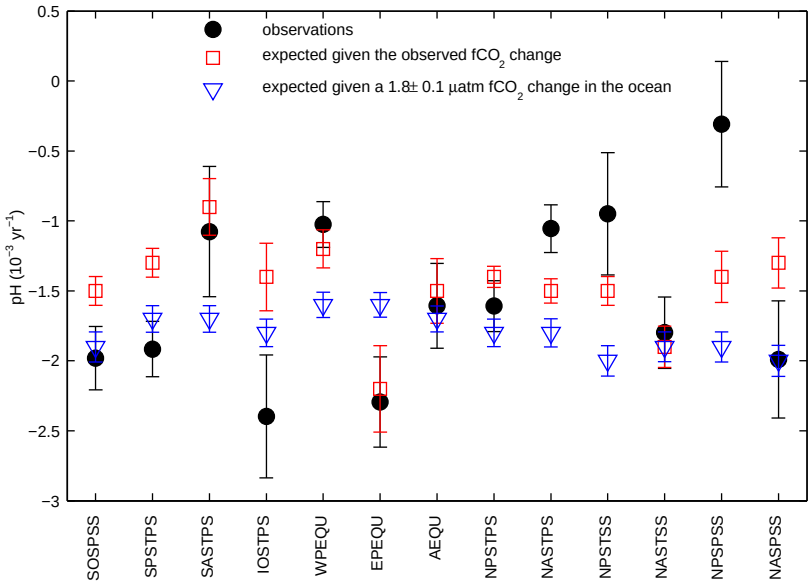
observations
expected given the observed fCO2 change
expected given a 1.8± 0.1 µatm fCO2 change in the ocean
pH (10−3 yr−1)
0.5
0
−0.5
−1
−1.5
−2
−2.5
−3
SOSPSS
SPSTPS
SASTPS
IOSTPS
WPEQU
EPEQU
AEQU
NPSTPS
NASTPS
NPSTSS
NASTSS
NPSPSS
NASPSS

Figure 6

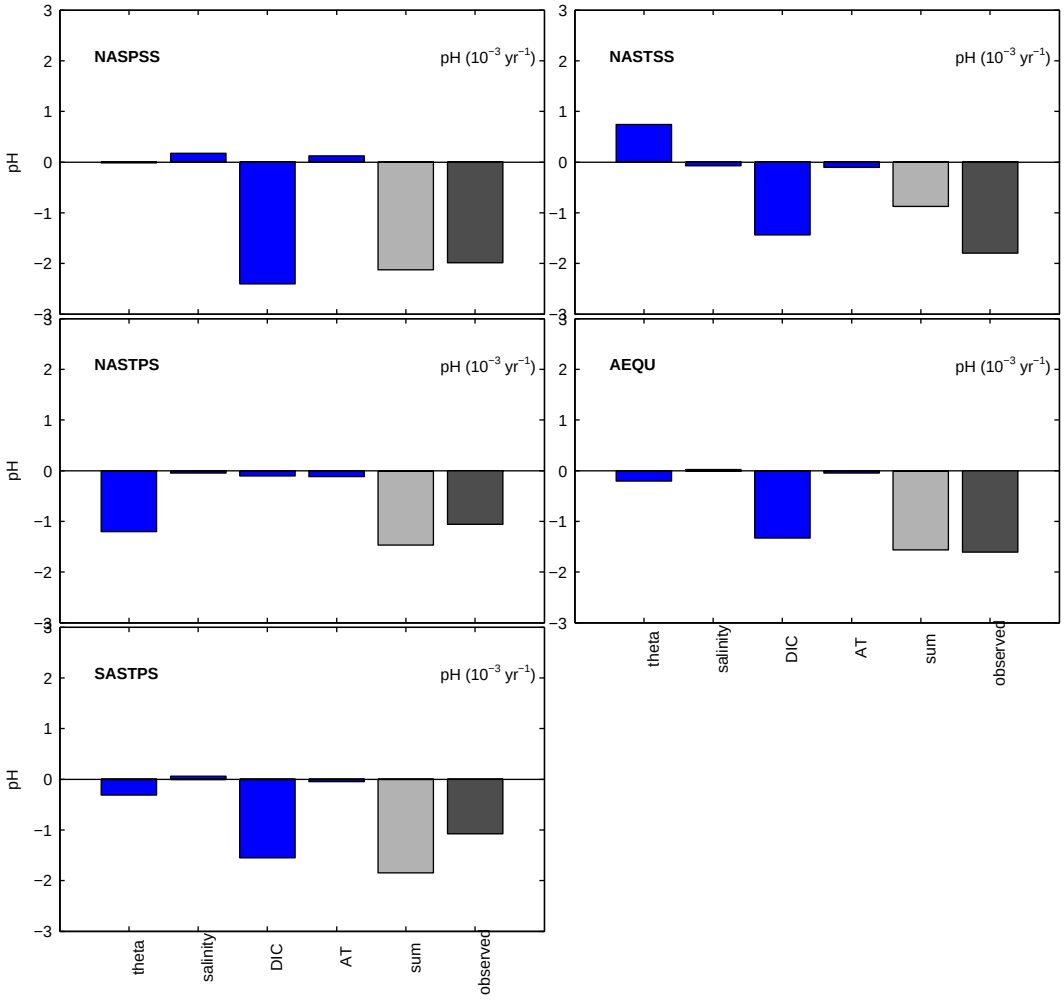
NASPSS
pH (10^{-3} yr^{-1})
NASTSS
pH (10^{-3} yr^{-1})
NASTPS
pH (10^{-3} yr^{-1})
AEQU
pH (10^{-3} yr^{-1})
SASTPS
pH (10^{-3} yr^{-1})
pH
3
2
1
0
−1
−2
−3
theta
salinity
DIC
AT
sum
observed

Figure 7

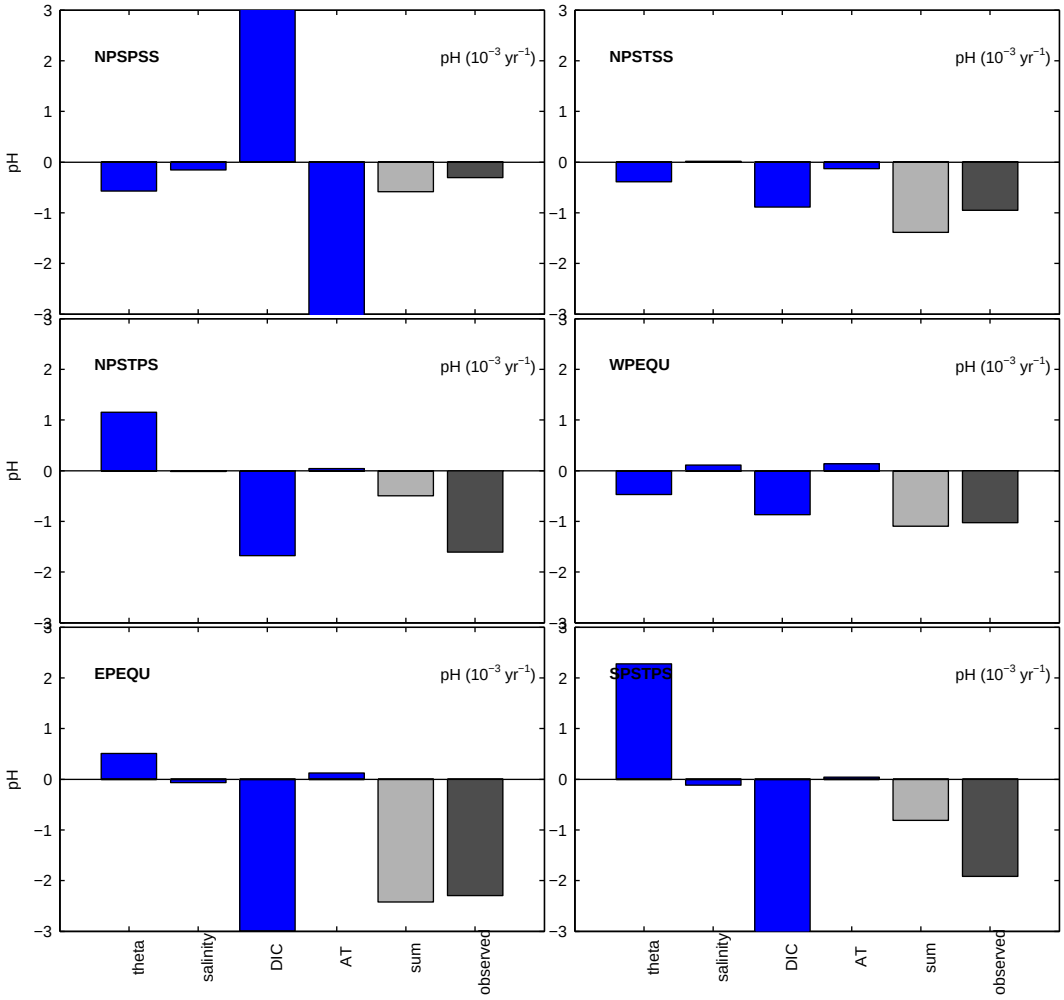
NPSPSS
NPSTSS
NPSTPS
WPEQU
EPEQU
SPSTPS
pH (10^{-3} yr^{-1})
pH
3
2
1
0
−1
−2
−3
theta
salinity
DIC
AT
sum
observed

Figure 8

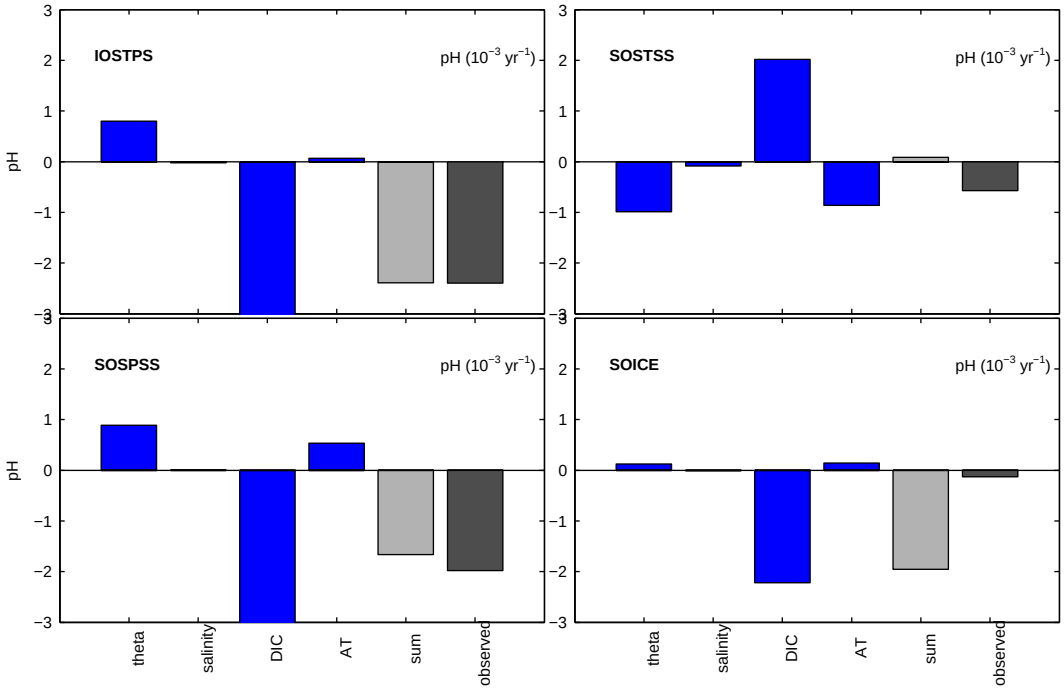
IOSTPS
SOSTSS
SOSPSS
SOICE
pH (10^{-3} yr^{-1})
pH
3
2
1
0
−1
−2
−3
theta
salinity
DIC
AT
sum
observed

Figure 9

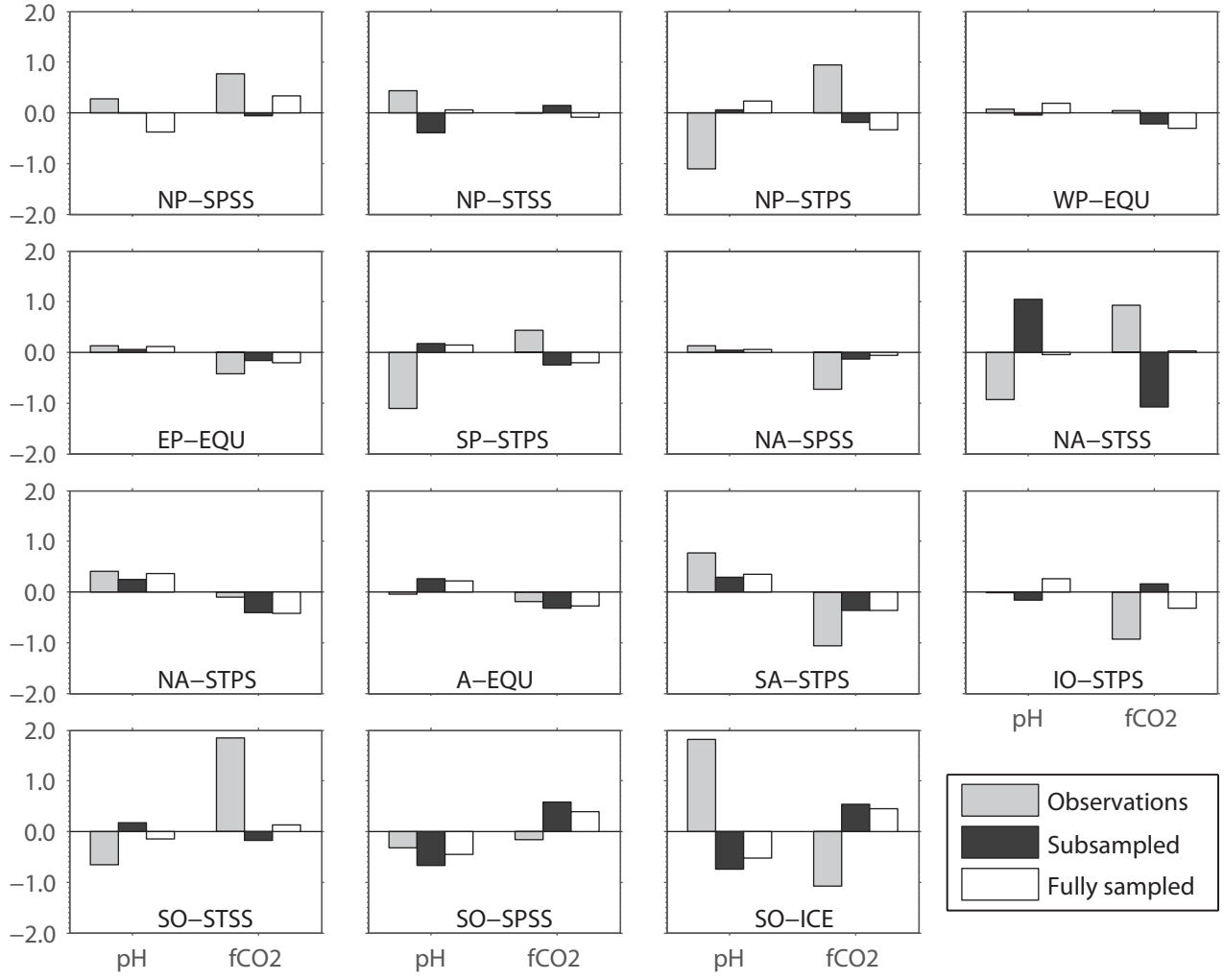
2.0
1.0
0.0
−1.0
−2.0
NP−SPSS
NP−STSS
NP−STPS
WP−EQU
EP−EQU
SP−STPS
NA−SPSS
NA−STSS
NA−STPS
A−EQU
SA−STPS
IO−STPS
SO−STSS
SO−SPSS
SO−ICE
pH
fCO2
Observations
Subsampled
Fully sampled

Figure 10